Zooplankton selectivity and nutritional value of phytoplankton influences a rich variety of dynamics in a plankton population model

Nandadulal Bairagi,[*] Suman Saha, Sanjay Chaudhuri, and Syamal Kumar Dana
Centre for Mathematical Biology and Ecology, Department of Mathematics, Jadavpur University, Kolkata 700032, India

(Received 1 August 2018; revised manuscript received 5 November 2018; published 8 January 2019)

Mathematical modeling may be an excellent tool to analyze and explain complex biological phenomena. In this paper, we use a mathematical model to reveal various interesting dynamical features of phytoplankton-zooplankton interaction and attempt to explain the reason for contrasting dynamics shown by different laboratory and field experiments. Our study shows that the phytoplankton-zooplankton interaction in a pelagic system is very complex and the plankton dynamics, including the bloom phenomenon, strongly depends on the selective predation of zooplankton and the nutritional value of phytoplankton. The study supports the existing hypothesis that decoupling at the plant-animal interface may occur due to strong fish predation on zooplankton. In addition, we argue that decoupling of the food chain may also occur under low to intermediate nutrient inflow if zooplankton feeds on phytoplankton having lower nutritional value. It is also shown that nutrient enrichment can destabilize an otherwise stable system if zooplankton feeds on highly nutritious prey, but unable to destabilize the system if zooplankton feeds on low-nutritious prey. This may be one possible explanation to the longstanding question: Why do some experiments show the *paradox of enrichment* and others do not?

DOI: 10.1103/PhysRevE.99.012406

I. INTRODUCTION

The planktonic food web is a very complex process that is still partially understood in spite of tremendous efforts given by researchers. Different factors have been identified that may affect the planktonic food web, namely, selective predation [1,2], nutrient inflow [3,4], grazing by higher predators [5], etc. Food selection is a natural characteristic of zooplankton [6], and its food selectivity criteria vary to a large extent [7]. When zooplankton is exposed to a variety of phytoplanktons, it selects a prey item depending on its size [8], digestibility [1], toxicity [9], availability [10–12], and nutrition value [1,13]. Several studies confirm that *Calanoid copepods* (zooplankton) can discriminate between toxic and nontoxic dinoflagellates [14], noxious and innoxious blue-greens [15], and live and dead algae of the same species [16]. Prey or food selectivity has significant impact on population stability [17]. Stoichiometric modulation of predation also shows contrasting dynamics in a pelagic system [18].

Different experiments confirm that a number of phytoplankton species have the ability to produce toxic substances (toxin-producing phytoplankton) and others do not (nontoxic phytoplankton). The toxin-producing phytoplanktons are sometimes less preferred or avoided by herbivorous zooplankton. In a recent work, Pal *et al.* [9] showed that the zooplankter (*Artemia salina*) can discriminate toxic phytoplankton (*Microcystis aeruginosa*) from the nontoxic phytoplankton (*Chaetocerous gracilis*). They observed that zooplankton is less inclined to opt for food based on size than the preferential selectivity for the safe nontoxic food species. It has also been demonstrated that the toxin produced by phytoplankton has widely differing effects on its grazers. Some zooplankton can digest or ingest toxin-producing phytoplankton without any harm, whereas some others experience deleterious effects [19].

Studies suggest that phytoplankton food quality for herbivorous zooplankton may play an important role in planktonic food web interactions in pelagic systems [1,2,13,44]. An optimal filter feeder selects foods based on their nutritional value. They first capture algae and then reject or ingest them after assaying their nutritional value [2]. In laboratory experiments, Demott [1] demonstrated that diet selection of *Eudiaptomus* spp. was strongly influenced by both algae quality and the availability of other foods. In particular, it was shown that discrimination against low-quality algae was strong enough in an abundance of high-quality algae, and weak when high-quality algae were scarce. Experiments also confirm that it can distinguish between the digestible and the digestion-resistant algae. In a recent work, Danielsdottir *et al.* [13] showed that phytoplankton biomass was suppressed and zooplankton can withstand strong predation pressure of zooplanktivory if the algal food quality is high. On the other hand, trophic decoupling at the plant-animal interface may occur if the food quality is low. The planktonic copepod *Acartia tonsa* has been demonstrated to exhibit prey-switching behavior depending on the availability of alternative preys [12].

These biological observations motivated us to study the dynamical behavior of the planktonic food web under the dual effect of zooplankton's selectivity and the nutritional value of phytoplankton. We use here a mechanistic predator-prey model that makes a balance between simplicity and realism so as to explain some of the observed behaviors, as cited above, from the dynamical system viewpoint. We incorporate in the model the effects of phytoplankton food quality as well as zooplankton's selectivity in an explicit way and then study

---

[*] nbairagi.math@jadavpuruniversity.in

their role in plankton dynamics and bloom phenomena. This bloom phenomenon is generally explained by a *bottom-up* approach, where nutrients are considered as a controlling factor of algal growth [20–22]. On the other hand, proponents of *top-down* approach believe that algal bloom is regulated by its grazer [23,24]. We verify the *bottom-up* and *top-down* controls under zooplankton's selectivity.

Some experimental results report that nutrient enrichment can reduce trophic transfer efficiencies between the plankton and its grazer [25] and may result in trophic decoupling [26,27]. In contrast, some other experiments show that trophic decoupling is unlikely due to nutrient enrichment [28,29]. So an important question is: Under what conditions does the planktonic ecosystem show trophic decoupling? Another puzzling phenomenon is the *paradox of enrichment* observed by Rosenzweig [30] in predator-prey interaction. According to this phenomenon, stability of phytoplankton-zooplankton interaction is lost with an increasing supply of nutrients [3,4,31], and populations become prone to extinction through high-amplitude oscillations. On the other hand, McCauley and Murdoch [32] reported that the *Daphnia*-algae (predator-prey) interaction does not show any nutrient-enriched cycle. Different explanations in favor of and against the paradox of enrichment have been reviewed in Ref. [33]. Here we propose and investigate a phytoplankton-zooplankton interaction model to provide insights into the trophic decoupling and the contradictory observations of the paradox of enrichment by presenting a broader scenario of the overall dynamics of the predator-prey species using the existing tools of nonlinear dynamics.

II. MODEL FORMULATION

A natural ecosystem consists of several types of phytoplankton, but for simplicity, we classify the entire phytoplankton population of a pelagic ecosystem into two categories: preferred phytoplankton (PP) and nonpreferred phytoplankton (NP). Phytoplanktons having superior nutrition value, easy digestibility, and nontoxicity are classified as PP, and phytoplanktons having inferior nutrition value, lower digestibility, and toxicity are considered as NP for planktivorous. Zooplankton selects phytoplankton depending on algal food quality, digestibility, toxicity, and availability. Phytoplankton's nutritional value is measured in terms of the reproductive gain of zooplankton. We assumed here that the toxin has either no effect on its grazer or has less nutritional value but never kills its grazers.

A predator's functional response, the relationship between prey density and feeding rate of the predator, is probably the most important component in a predator-prey model. Since zooplankton feeds on both PP (denoted by p_1) and NP (denoted by p_2) with some preference for PP over NP, multiple-prey type II response functions [34,35] $n\theta p_1/(a+\theta p_1+p_2)$ and $np_2/(a+\theta p_1+p_2)$ have been considered for PP and NP, respectively. The dimensionless parameter θ measures the selectivity or preference of zooplankton, which is the ratio of attack rates on PP over NP. In particular, if $\theta > 1$ then zooplankton prefers PP; $\theta = 1$ implies equal preference for PP and NP; and $0 < \theta < 1$ means that zooplankton prefers NP. Here we assume that the reproductive gain from PP is higher than that of NP. The grazing of zooplankton by a fish population is considered to be proportional to the density of zooplankton and that of the fish population. Since the generation time of a fish population is significantly higher than that of zooplankton, we consider fish as a static predator, and hence their density is treated as a constant instead of a variable.

Assuming that zooplankton consumes both PP and NP with some preference for PP over NP, we propose the following model for the PP-NP-zooplankton interaction:

$$\begin{aligned}\frac{dp_1}{dt} &= r_1p_1\left(1-\frac{p_1}{k_1}\right)-\alpha_1p_1p_2\\&\quad-\frac{n\theta p_1z}{a+\theta p_1+p_2},\qquad P_1(0)>0,\\\frac{dp_2}{dt} &= r_2p_2\left(1-\frac{p_2}{k_2}\right)-\alpha_2p_1p_2\\&\quad-\frac{np_2z}{a+\theta p_1+p_2},\qquad p_2(0)>0,\\\frac{dz}{dt} &= \frac{\xi_1n\theta p_1z}{a+\theta p_1+p_2}+\frac{\xi_2np_2z}{a+\theta p_1+p_2}\\&\quad-d_1z,\quad z(0)>0.\end{aligned}\tag{1}$$

Here $p_1(t)$, $p_2(t)$, and $z(t)$ are, respectively, the concentrations of PP, NP, and zooplankton populations at time t. Phytoplankton and zooplankton densities are measured in mg $c\,l^{-1}$. Both PP and NP grow logistically to their respective carrying capacities k_1 and k_2 with intrinsic growth rates r_1 and r_2; α_1 and α_2 are the interspecific competition coefficients. The parameters ξ_1 and ξ_2 represent the reproductive gains of zooplankton from PP and NP, respectively, where $0 < \xi_2 \leqslant \xi_1 < 1$. The total background mortality rate of zooplankton is measured by the composite parameter d_1, where $d_1 = d + D$. Here d is the natural mortality rate of zooplankton, and D is the additional mortality rate, if any, due to fish predation. We have considered a homogeneous mixture of phytoplankton-zooplankton populations for simplicity and ignored heterogeneities and the patchiness of the plankton population. We have also not considered the transport of a plankton population by flow or turbulence of water, a salient characteristic of ocean water.

III. PARAMETER SELECTION

Most of the system parameters (see Table I) are selected from similar models [36–38] studied for phytoplankton-zooplankton interactions, and a few are determined by our analytical results (see Table II). In the *Daphnia*-algal model, Murdoch *et al.* [36] observed limit cycles (paradox of enrichment) for modest environmental carrying capacity 0.5 mg $c\,l^{-1}$ for algae, and we therefore set this value as our default value for the parameter k_1. To account for different sizes of preferred and nonpreferred phytoplanktons, carrying capacity of nonpreferred phytoplanktons (k_2) has been considered nonidentical and is set as 0.4 mg $c\,l^{-1}$. However, as demonstrated later, the dynamics does not vary if one relaxes this assumption and considers $k_1 = k_2$. Genkai-Kato and Yamamura [37]

TABLE I. Parameter description and their values with references.

Parameter description	Default value	Ref.
r_1 = Intrinsic growth rate of preferred phytoplankton	0.5 per day	[36]
r_2 = Intrinsic growth rate of nonpreferred phytoplankton	0.25 per day	[37]
k_1 = Carrying capacity of preferred phytoplankton	0.5 mg $c\ l^{-1}$	[36]
k_2 = Carrying capacity of nonpreferred phytoplankton	0.4 mg $c\ l^{-1}$	Selected
α_1 = Interspecific competition coefficient of preferred phytoplankton	0.1	[37]
α_2 = Interspecific competition coefficient of nonpreferred phytoplankton	0.4	[37]
n = Maximum nonpreferred prey capture rate	0.435 per day	[38]
a = Half-saturation constant	0.16 mg $c\ l^{-1}$	[36]
ξ_1 = Reproductive gain from preferred phytoplankton	0.5	[36,37]
ξ_2 = Reproductive gain from nonpreferred phytoplankton	0.28	Selected
d_1 = Background mortality of zooplankton	0.12 per day	[36]
θ = Selectivity of zooplankton	0.5/2	Selected

considered the intrinsic growth rates of palatable and unpalatable preys for zooplankton as 0.5 and 0.25. Harmful algae are assumed to have a slower growth rate than nonharmful algai ($r_2 < r_1$) [37,39], and more profitable phytoplankton is assumed to be a superior competitor than less profitable phytoplankton ($\alpha_1 < \alpha_2$) [37]. Comparing our model with that of Genkai-Kato and Yamamura [37], we set the default values of r_1 and r_2 as 0.5 and 0.25 per day, respectively, and that of α_1 and α_2 as 0.1 and 0.4, respectively. Maximum prey capture rate was estimated as 0.435 d^{-1} in Ref. [38], and we therefore set this value for n. The value of half-saturation constant, a, is fixed at 0.16 mg $c\ l^{-1}$ following Ref. [36]. The natural death rate of zooplankton is set as $d = 0.12$, which considers the minimum mortality rate in field (0.03/day) and respiration (maintenance) rate (0.09/day) [36]. Death due to fish predation (D) is initially set at 0, giving the default background mortality of zooplankton as $d_1 = 0.12$. Here D will be varied from 0 (no fish predation) to 0.24 (maximum rate of fish predation) to test the variational effect of fish predation. For these values of parameters, we determine two critical values (see Table II) as $\frac{d_1}{n} = 0.2759$ and $\alpha_2 K_1 = 0.2$. Thus, from stability results (see Table II), the NP- and zooplankton-free equilibrium E_1 is locally asymptotically stable whenever $\xi_1 < 0.2759$ and $r_2 < 0.2$. Similarly, the PP- and zooplankton-free equilibrium E_2 is locally asymptotically stable if $\xi_2 < 0.2759$ and $r_1 < 0.04$. If any of E_1 and E_2 is stable, then other equilibrium points (E_3, E_4, E_5, E^*) do not exist. We therefore assume in the subsequent simulations that ξ_1, ξ_2 and r_1, r_2 always assume values higher than their respective critical values. We set the nutritional value of PP to its maximum value $\xi_1 = 0.5$ [36,37] and that for NP to its lowest value $\xi_2 = 0.28$. Assuming that nutrition value of NP never exceeds that of PP, we shall vary ξ_2 from the minimum value 0.28 to the maximum value 0.5 to test the variational effect of nutritional value of phytoplankton. The intrinsic growth rate of PP is set at its maximum value 0.5 [36] and that for NP is set to its minimum value 0.25 [37]. We thus make our default parameter set as in Table I so that equilibrium points E_3, E_4, E_5, and E^* do exist.

IV. RESULTS

A. Analytical results

The model system (1) has seven equilibrium points, E_i ($i = 0, 1, 2, 3, 4, 5$) and E^*, whose existence and stability conditions are summarized in Table II (see Secs. I– II of the Supplemental Material [40] for analytical proof). Hopf bifurcation analysis about the equilibrium points E_4, E_5, and E^* with respect to different parameters are also presented there.

B. Numerical simulations

Our objective is to explore the variety of dynamics of the system (1) under the influence of parameters that measure the zooplankton's selectivity or preference and the nutritional value of phytoplankton. We use the Runge-Kutta fourth-order algorithm with a step size 0.01. Initial value is kept fixed at $(p_{10}, p_{20}, z_0) = (0.3065, 0.0161, 0.0330)$ for each simulation, if not otherwise stated.

TABLE II. Sufficient conditions for the existence and stability of different equilibrium points (existence conditions are written in normal face and stability conditions are in boldface).

Equilibria	Coordinates	Stability conditions
E_0	(0,0,0)	Always unstable
E_1	$(k_1, 0, 0)$	$\boldsymbol{r_2 < \alpha_2 k_1, \quad \xi_1 < d_1/n}$
E_2	$(0, k_2, 0)$	$\boldsymbol{r_1 < \alpha_1 k_2, \quad \xi_2 < d_1/n}$
E_3	$(\bar{p}_1, \bar{p}_2, 0)$	$r_1 > \alpha_1 k_2, \quad r_2 > \alpha_2 k_1,$ $\boldsymbol{\xi_1 < d_1/n, \quad \xi_2 < d_1/n}$
E_4	$(\hat{p}_1, 0, \hat{z})$	$\xi_1 > \frac{d_1}{n}, \quad \frac{a d_1}{k_1(\xi_1 n - d_1)} < \theta < \mathbf{min}[\boldsymbol{\frac{a(\xi_1 n + d_1)}{k_1(\xi_1 n - d_1)}, \frac{a\alpha_1\alpha_2}{r_2(\xi_1 n - d_1)}}]$
E_5	$(0, \tilde{p}_2, \tilde{z})$	$\frac{d_1}{nk_2}(k_2 + a) < \xi_2 < \mathbf{min}[\boldsymbol{\frac{d_1}{n}(\frac{k_2+a}{k_2-a}), \frac{d_1}{nr_1}(r_1 + a\alpha_1)}]$
E^*	(p_1^*, p_2^*, z^*)	$\xi_1 > \frac{d_1}{n}, \quad \xi_2 > \frac{d_1}{n}, \quad \frac{r_1}{\alpha_2 k_1} < \theta < \min[\frac{r_1}{r_2}, \frac{r_2}{r_1}, \frac{\alpha_1 k_2}{r_2}],$ $r_2 p_2^* + \alpha_2 k_2 p_1^* < r_2 k_2,$ $\mathbf{F_1 > 0, \quad F_3 > 0, \quad F_1 F_2 - F_3 > 0}$

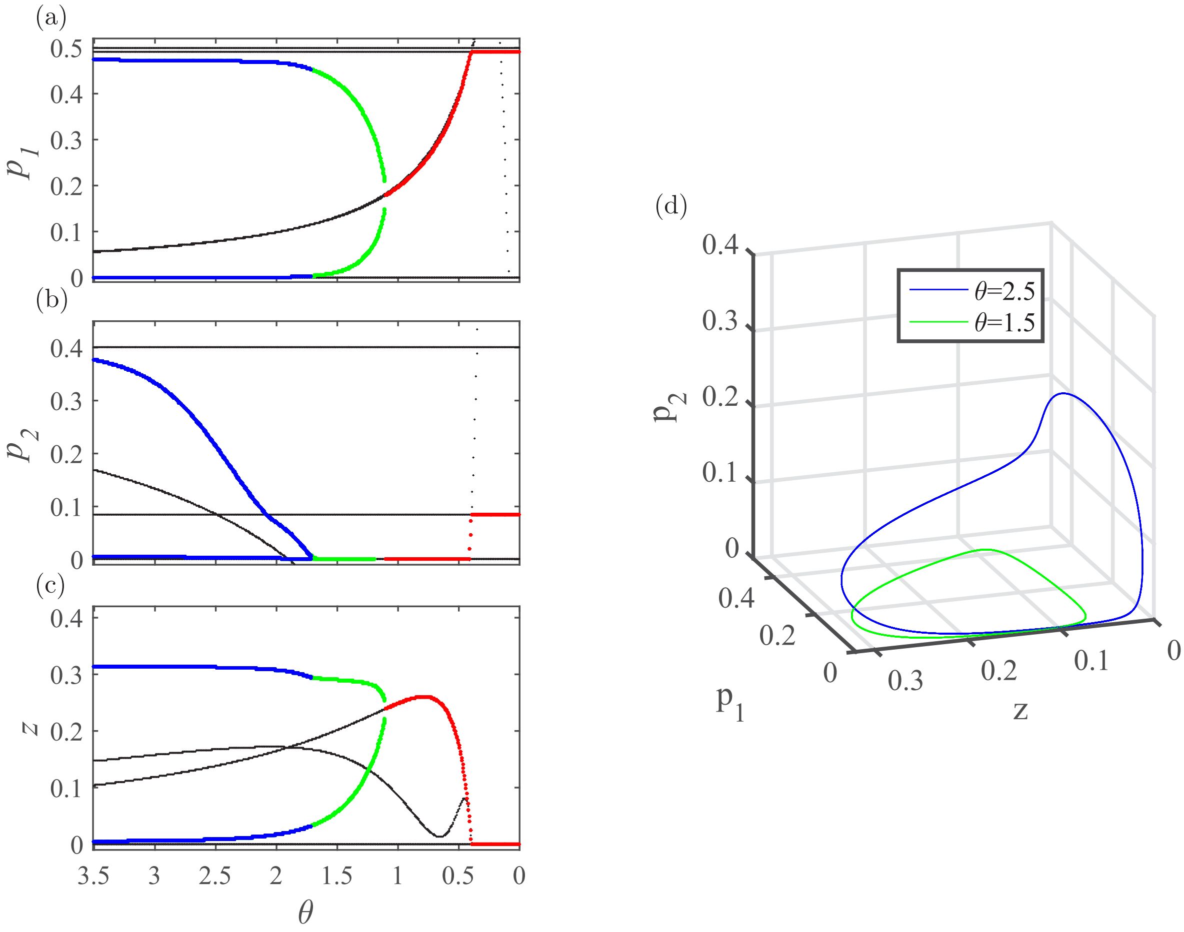

FIG. 1. Bifurcations of plankton dynamics against preference parameter θ in panels (a)–(c). Five distinct varieties of dynamical behaviors are seen as θ varies: (1) three populations p_1, p_2, and z coexist in oscillatory states (blue line) for $\theta > 1.712$, (2) p_1 and z coexist in oscillatory states [green lines in panels (a) and (c)] but p_2 goes to extinction [green line in panel (b)] in the range $1.1077 < \theta < 1.712$, (3) NP-free equilibrium E_4 is stable (red line) for $\theta \in (0.4144, 1.1077)$ where p_1 and z have constant densities but p_2 has zero density, (4) three species coexist at steady states in a smaller range $0.4144 < \theta < 0.3975$, and (5) zooplankton-free equilibrium E_3 is stable for $0 < \theta < 0.4144$, where p_1 and p_2 have constant densities and z has zero density. Red dotted lines represent stable fixed points, green and blue lines for the limit cycle and, black dots represent unstable fixed points. A transcritical bifurcation of the limit cycle is depicted by the transition from the blue to green line at $\theta = 1.712$. The junctions of green and red lines indicate the Hopf bifurcation point at $\theta = 1.1077$. A first transcritical bifurcation of fixed point occurs at $\theta = 0.4144$, where the NP population p_2 revives from extinction and all species coexist in steady state for a shorter range. At $\theta = 0.3975$, a second transcritical bifurcation of fixed point occurs when z goes to extinction and NP (p_2) maintains a low density along with high density of PP (p_1). (d) The 3D trajectory of all species more clearly depicts the transcritical bifurcation of a limit cycle. The trajectory in the green line lies on $p_2 = 0$ plane, but the trajectory in blue shows the coexistence of all three species, indicating an exchange of stability of the limit cycles. Parameters are as in Table I except θ. No fish predation is considered, i.e., $D = 0$.

1. Effect of zooplankton's selectivity

First, we present a broader picture of the plankton dynamics by varying the zooplankton selectivity (preference) parameter θ. Distinct varieties of dynamics with disparate features of population bloom emerge with a varying θ as shown in Figs. 1(a)–1(c) with their critical transitions. When zooplankton strongly selects PP (for $\theta > 1.712$), all three populations coexist in oscillatory states as shown in Figs. 1(a)–1(c) (blue lines). At the critical point $\theta = 1.712$, a transcritical bifurcation of the limit cycle occurs when the NP population (p_2) is suppressed and eventually dies out while other two populations still coexist and oscillate around the unstable fixed point E_4 (green line). This transition is more clearly visible in Fig. 1(d) where a three-dimensional (3D) trajectory on the $p_2 = 0$ plane (green line) is shown for $\theta = 1.5$ along with another trajectory (blue line) of all coexisting populations for $\theta = 2.5$ that actually pops up from $p_2 = 0$ plane via the transcritical bifurcation of the limit cycle at $\theta = 1.712$. By lowering the preference on p_1, the stable oscillatory state [blue line in Fig. 1(d)] becomes unstable, whereas another coexisting unstable limit cycle transits to a stable limit cycle (green line). Reduction of zooplankton's grazing on p_1 by lowering the θ value leads to extinction of p_2 for $\theta \leqslant 1.712$. Zooplankton though feeds dominantly on p_1, the nonpreferred phytoplankton p_2 cannot survive as they are inferior competitor to p_1. At another critical value $\theta = 1.1077$, the system undergoes a reverse Hopf bifurcation around E_4 and transits to a steady state [red dotted line in

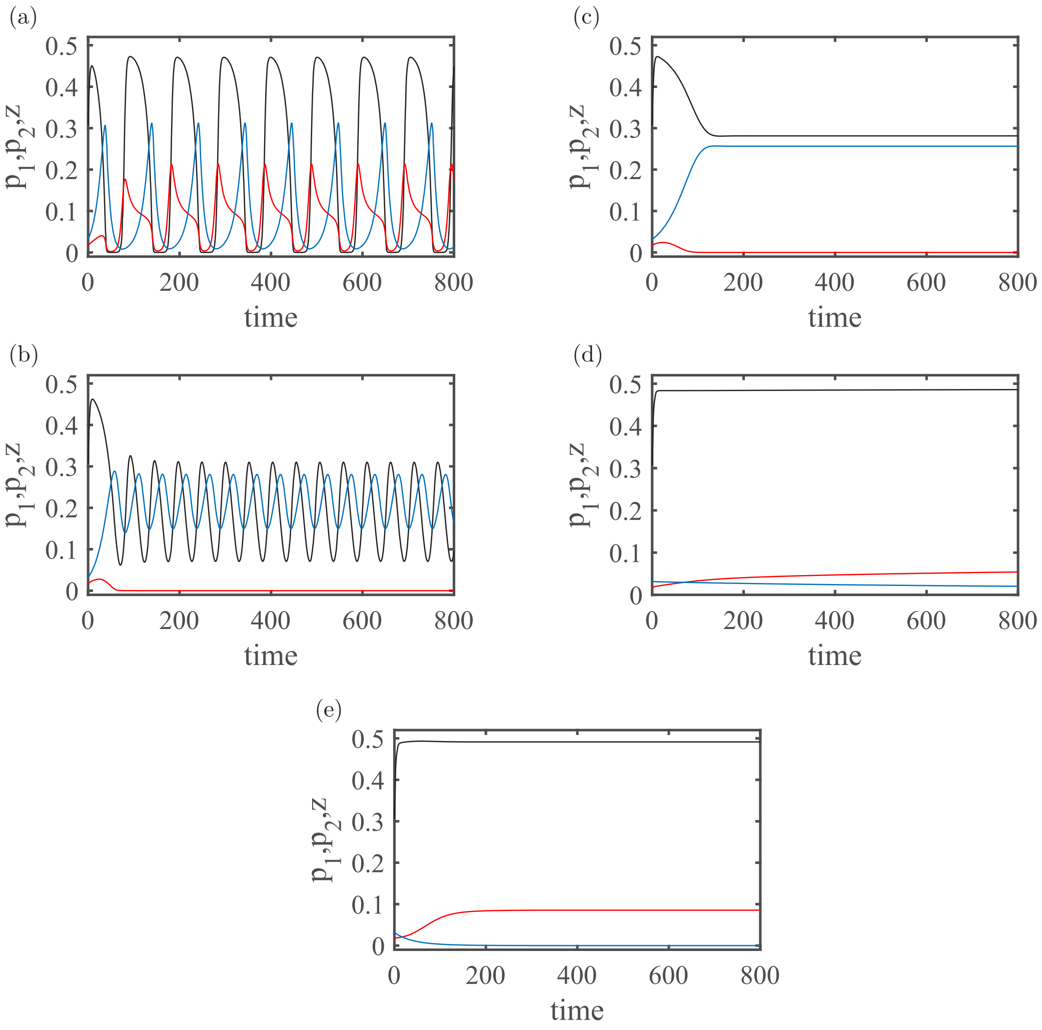

FIG. 2. Variety of temporal dynamics of plankton population in system (1) for particular values of preference parameter θ. The populations of p_1, p_2, and z are shown in black, red, and blue lines, respectively. As θ varies from higher to lower values, the system exhibits (a) relaxation oscillation around E^* when all three populations oscillate for $\theta > 1.712$, (b) regular oscillation around E_4 where PP and zooplankton oscillate but NP goes to extinction for $1.712 \geqslant \theta > 1.1077$, (c) E_4 is stable where PP and zooplankton have constant density but NP goes to extinction, for $0.4144 < \theta < 1.1077$, (d) three species coexist in a stable steady state E^* for $0.3975 < \theta < 0.4144$, and (e) E_3 is stable where PP and NP have constant density yet zooplankton goes to extinction, for $0 < \theta < 0.3975$. Parameters are considered as given in Fig. 1.

Figs. 1(a)–1(c)], where the equilibrium point E_4 becomes stable. As the preference parameter goes below the Hopf bifurcation point at $\theta = 1.1077$, biomass of p_1 gradually increases while p_2 remains at zero population density. NP population p_2 starts reviving from extinction at $\theta = 0.4144$ via transcritical bifurcation of the stable fixed point E_4, but the coexistence equilibrium point E^* becomes stable up to the value of $\theta = 0.3975$. Below $\theta = 0.3975$, both PP and NP coexist in stable states, and the predator-free equilibrium E_3 becomes stable. Since zooplankton is strongly inclined to low nutritious phytoplankton (p_2), high-density zooplankton cannot sustain on it and goes to extinction. In the absence of zooplankton, NP revives and coexists in a stable state with high-density superior competitor PP, indicating the bloom of preferred phytoplankton as seen in Figs. 1(a)–1(c).

Transitions to varieties of dynamical behaviors of the plankton populations are revealed in Fig. 1, which are further elaborated by their respective temporal dynamics in Fig. 2. Three species coexist in oscillatory states as shown in Fig. 2(a) for $\theta > 1.712$, and it reveals a distinctive dynamical feature that the oscillations are basically of relaxation type. Both phytoplanktons (p_1 and p_2) bloom simultaneously at a faster rate, and then their populations relax together at a slower rate to a steady state when the zooplankton (z) actually blooms out of phase with the phytoplanktons, and this feature repeats in time. In other words, the z bloom always lags the p_1 and p_2 bloom in time. Noticeably, p_2 has a slower rate of relaxation than p_1. Figure 2(b) reveals the temporal dynamics after the transcritical bifurcation of the limit cycle at $\theta = 1.712$ when the species p_2 dies out (red line) and other two (p_1 and z in black and blue lines, respectively) are still blooming in periodic oscillatory states; no relaxation-type oscillation exits in this case. However, they still show a lag in blooming. This transition from a relaxation-type oscillation to a partially oscillatory state, and that too with a simple periodic oscillation is a unique feature of the model. How two timescales in the

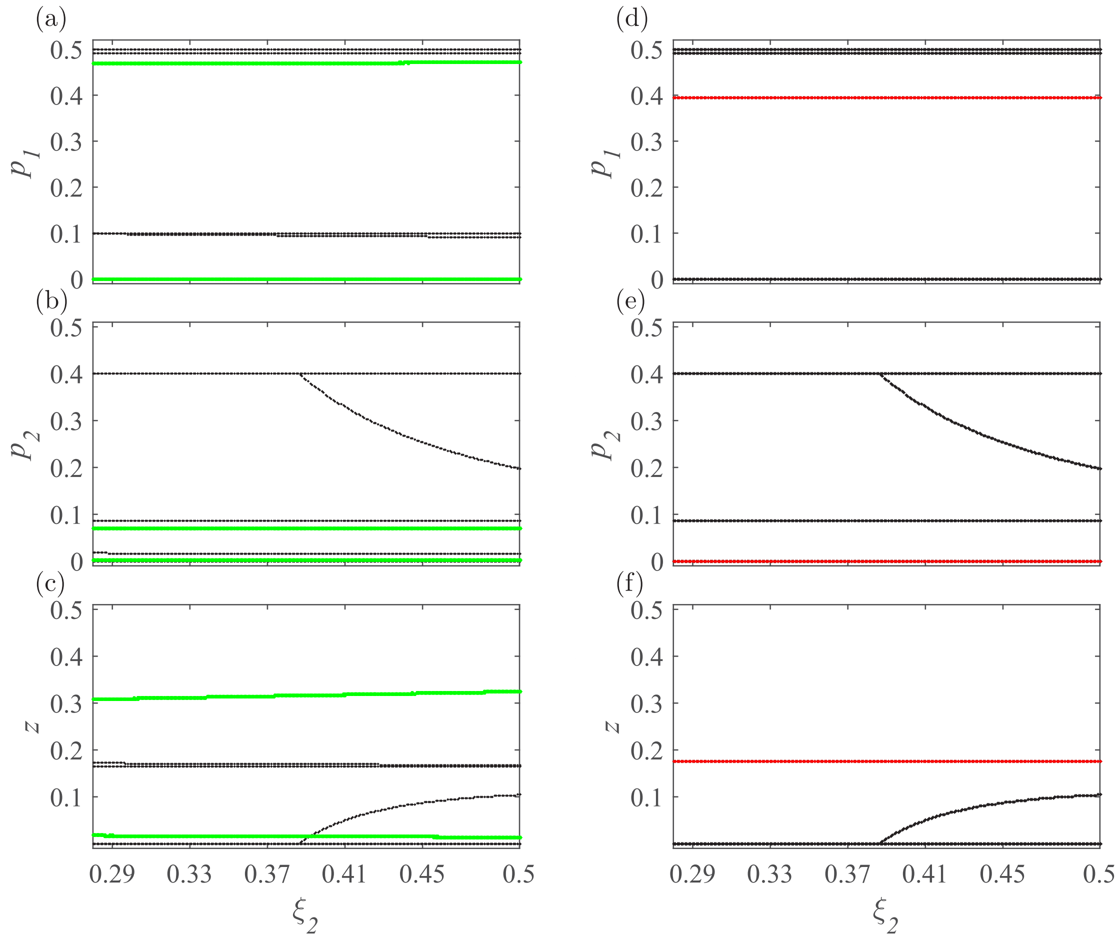

FIG. 3. Biomass change with nutritional value of NP when zooplankton feeds on PP ($\theta = 2$) is presented in left panels. Right panels show the biomass change with nutritional value of NP when zooplankton feeds on NP ($\theta = 0.5$). Green lines indicate maxima and minima of oscillatory dynamics, red lines for stable steady states, and black lines for unstable steady states. Parameters are as in Table I except ξ_2. No fish predation is considered ($D = 0$).

relaxation-type oscillations emerge and then disappear with a suppression of oscillation in one variable for the change in a single parameter is quite interesting from a purely dynamical system viewpoint. Then the system (1) transits to steady-state dynamics showing three distinctly different states of coexistence, as shown in Figs. 2(c)–2(e), in the lower ranges of preference parameter $1.1077 > \theta > 0.4144, 0.4144 > \theta > 0.3975$, and $0.3975 > \theta > 0$, respectively. Interestingly, the nonpreferred phytoplankton (p_2) cannot survive even when zooplankton is inclined to preferred phytoplankton (p_1), as p_2 is assumed to be an inferior competitor as well as a slow-growing species. When zooplankton shifts its feeding preference from PP to NP (the case $\theta < 1$), the zooplankton population gradually declines from its high biomass and eventually goes to extinction due to starvation. A stable coexistence of all three species, however, can be observed [see Fig. 2(d)] for a narrow range of preferred parameter, $0.394 < \theta < 0.4144$. For the preference value $\theta < 0.3975$, NP revives in absence of zooplankton and coexists in a stable state with PP biomass as shown in Fig. 2(e). Thus a decoupling of food chain may occur at the plant-animal interface if zooplankton feeds on low-nutritious phytoplankton.

2. Effect of phytoplankton's nutritional value

Next we focus on the effects of nutritional value (ξ_2) of NP (p_2) on the plankton dynamics. Once again, we show the variation of species population in bifurcation diagrams (Fig. 3) by varying ξ_2 within its permissible range 0.28 to 0.5. Note that ξ_2 decides the reproductive gain of zooplankton and thereby represents the nutritional value of p_2. We consider two situations: (1) zooplankton strongly selects p_1 and (2) zooplankton strongly selects p_2. For a stronger preference to p_1, we assign $\theta = 2$, which is twice as large than the case of equal preference ($\theta = 1$). Alternatively, to mean a stronger preference to p_2, we assign a lower value $\theta = 0.5$, which is twofold lower than the equal preference. When zooplankton strongly feeds on p_1, cyclic coexistence (oscillatory dynamics) of all species is the only outcome [see Figs. 3(a)–3(c)] as the nutritional value of p_2 is varied within the prescribed range ($0.28 < \xi < 0.5$). On the contrary, if zooplankton strongly feeds on p_2 ($\theta = 0.5$), NP cannot survive [see Figs. 3(d)–3(f)] in the same range of ξ. Zooplankton, however, survives with a weaker feeding on p_1 at lower density where the NP-free equilibrium E_4 is stable.

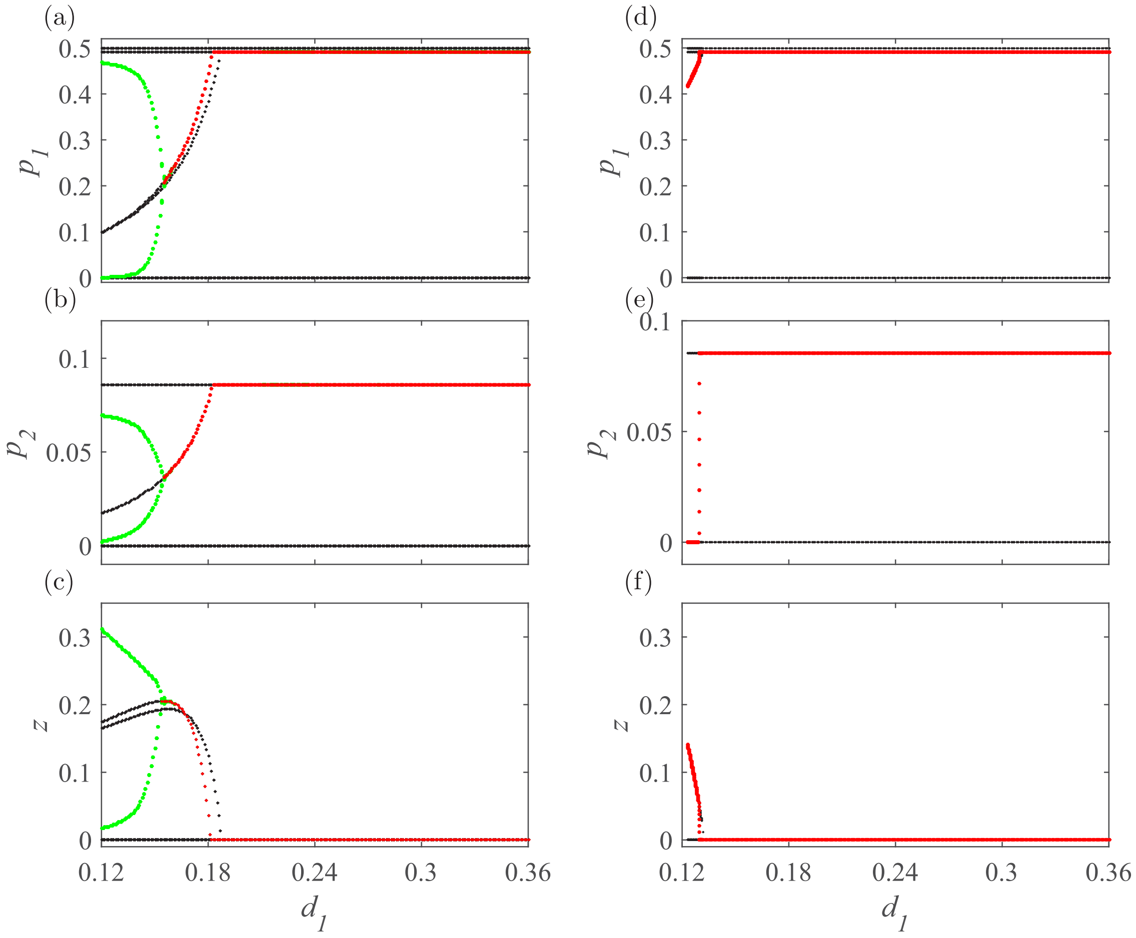

FIG. 4. Plankton dynamics under two different preferences when the removal rate of zooplankton augmented by fish predation is varied. Figures in the left panel show the dynamics when zooplankton is inclined to PP ($\theta = 2$) and in the right panel represent the same when zooplankton is inclined to NP ($\theta = 0.5$). Green line indicates oscillatory state; red and black dots indicate stable and unstable steady states, respectively. A reverse Hopf bifurcation occurs at the junction of the green line and red dots at $d_1 = 0.1574$, and a transcritical bifurcation occurs at $d_1 = 0.1861$ [see panels (a)–(c)]. Figures in the right panel show two consecutive transcritical bifurcations at $d_1 = 0.1293$ (transition from E_4 to E^*) and $d_1 = 0.1391$ (transition from E^* to E_3). Parameters are as in Table I except d_1.

3. *Effect of fish predation*

So far we have ignored the effect of fish predation. However, zooplanktivorous fish population has significant effect on plankton food web dynamics, which we illustrate here. We vary the zooplankton's removal rate d_1 from its base line value 0.12 (where removal rate of zooplankton by fish population is zero, $D = 0$ and $d = 0.12$) to its maximum value 0.36 (where fish predation is maximum, $D = 0.24$ and $d = 0.12$). The test is performed again under two situations of zooplankton's selectivity: (1) $\theta = 2$, where zooplankton prefers p_1 [Figs. 4(a)–4(c)] and (2) $\theta = 0.5$, where zooplankton prefers p_2 [Figs. 4(d)–4(f)]. All three species oscillate around the interior fixed point E^* if zooplankton is strongly inclined to p_1 and the augmented removal rate of zooplankton is very low ($0.12 < d_1 < 0.1574$). In fact, this behavior is also observed when there is no fish predation, i.e., $d_1 \leqslant 0.12$. A transition to stable E^* is observed via reverse Hopf bifurcation at the junction of green lines and red dotted lines ($d_1 = 0.1574$) as seen in Figs. 4(a)–4(c). Stable coexistence of all three species is observed with increasing fish predation ($0.1574 < d_1 < 0.1861$), but with a diminishing biomass of zooplankton. Zooplankton goes to extinction when grazing pressure is too intense ($d_1 > 0.1861$). In this latter case, the equilibrium E_3 becomes stable as E^* loses its stability via transcritical bifurcation and both phytoplanktons coexist in stable states. The biomass of p_1, however, is significantly higher than of p_2 since it is a superior competitor. The dynamics is simpler when zooplankton feeds on NP (p_2) for $\theta = 0.5$ as shown in the Figs. 4(d)–4(f). For $0.12 < d_1 < 0.1293$, p_2 goes to extinction, but revives after $d_1 > 0.1293$ through a transcritical bifurcation at $d_1 = 0.1293$. All populations may coexist in stable steady state in a very narrow range of fish predation ($0.1293 < d_1 < 0.1391$). As fish predation increases, zooplankton cannot survive on low nutritious p_2 and goes to extinction via a second transcritical bifurcation at $d_1 = 0.1391$. Thus, a decoupling of food chain may occur at the plant-animal interface under both types of preferences due to intense fish predation, supporting previously observed results [5]. Both types of phytoplankton, in this case, reach equilibrium densities of E_3, indicating plankton bloom [41].

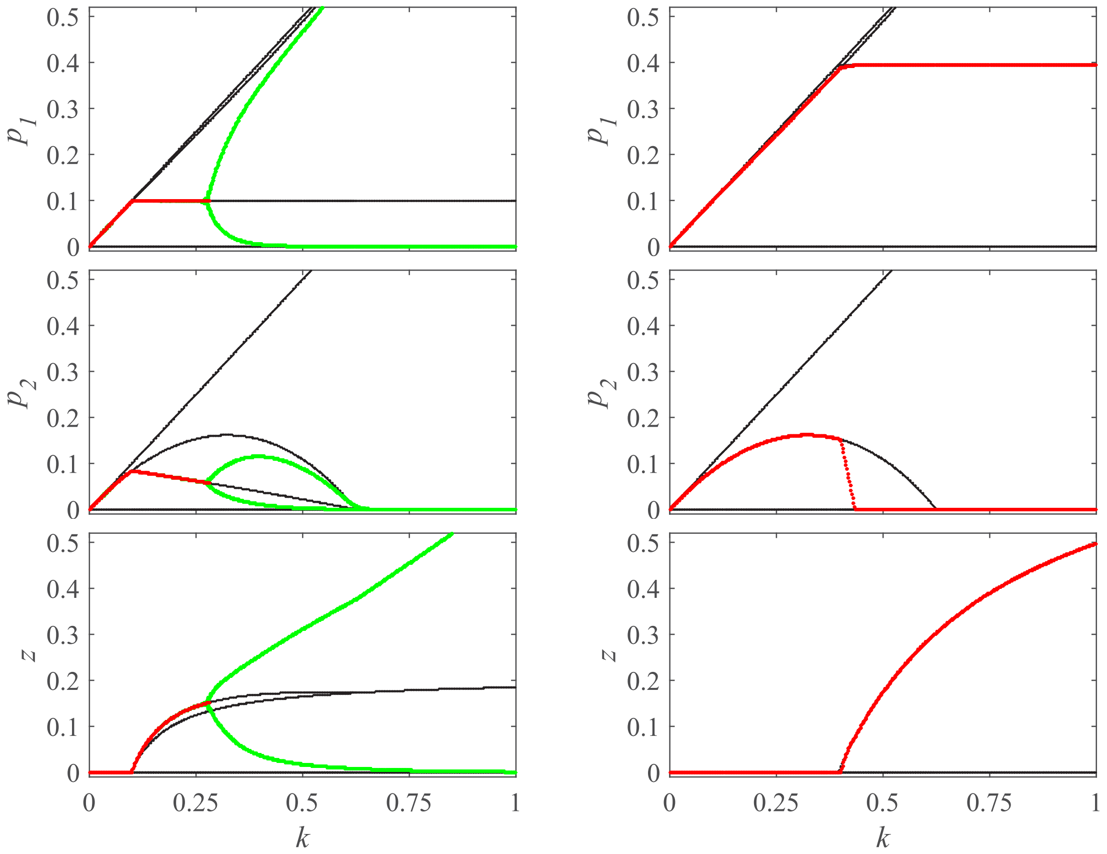

FIG. 5. Bifurcation of plankton (p_1, p_2, and z) dynamics with nutrient variation under two preferences of zooplankton: $\theta = 2$ (left panels) and $\theta = 0.5$ (right panels). Green lines indicate a stable oscillatory state; red and black dots denote stable and unstable steady states, respectively. Recurrence multispecies bloom are the most probable outcomes of the system when zooplankton prefers PP ($\theta = 2$) with increasing nutrient availability. If zooplankton prefers NP ($\theta = 0.5$), then zooplankton-free stable state or NP-free stable state are the most likely cases as nutrient inflow is increased. Parameters are as in Table I except $k_1 = k_2 = k$.

4. Effect of nutrient enrichment

Finally, we discuss the effect of nutrient enrichment on our model system. We do it, following the conventional approach, by increasing the environmental carrying capacity [36,37]. For simplicity, it is assumed here that the carrying capacities of both types of phytoplankton are the same ($k_1 = k_2 = k$) and increase at the same rate with nutrient availability. We therefore vary the parameter k from a very low nutrient input to a high nutrient input ($k = 1$). We explored both the possibilities, as our declared objective earlier, a strong preference either to PP ($\theta = 2$) or NP ($\theta = 0.5$) and presented our results in the left and right panels of Fig. 5, respectively. For a very low nutrient input, the zooplankton-free equilibrium point E_3 is stable up to the transcritical bifurcation point $k = 0.09854$. All populations coexist in the stable steady state (E^*) as the nutrient availability increases ($0.09854 < k < 0.2814$). The coexistence equilibrium E^* undergoes a Hopf bifurcation at $k = 0.2814$, and all three species coexist in oscillatory states for the range $0.284 < k < 0.649$. Further nutrient input ($k > 0.6249$) causes larger oscillations in PP and zooplankton. The inferior competitor p_2, however, cannot survive with high-density superior competitor p_1 and goes to extinction through a transcritical bifurcation of limit cycle at $k = 0.6249$. Preferred phytoplankton (p_1) and zooplankton (z) maintain their growing amplitude with increasing nutrient input. Thus, eutrification is the causative factor of algal growth and recurrence bloom. This result supports the existing hypothesis of the paradox of enrichment, namely, stable equilibrium becomes unstable with high-amplitude oscillations with increasing nutrient supply [30]. In the other case, when zooplankton feeds on NP ($\theta = 0.5$), the zooplankton-free equilibrium point E_3 becomes stable up to $k = 0.4004$ (see the figures in the right panel). Thus, decoupling may occur at the plant-animal interface even under a moderately high nutrient input if zooplankton feeds on low-nutritious phytoplankton. For a long range of higher nutrient inflow ($k > 0.4004$), the preferred phytoplankton (p_1) and zooplankton (z) coexist in stable equilibrium state and no paradox of enrichment is observed, supporting the observation of McCauley and Murdoch [32]. Here zooplankton mainly consumes slow growing less nutritious phytoplankton p_2, it cannot maintain the increasing biomass of zooplankton and goes to extinction, making the equilibrium E_4 stable through a transcritical bifurcation at $k = 0.4004$.

5. Phase diagram: Two-parameter bifurcation

We present a broader scenario of dynamical changes in our plankton food web model when two parameters are varied

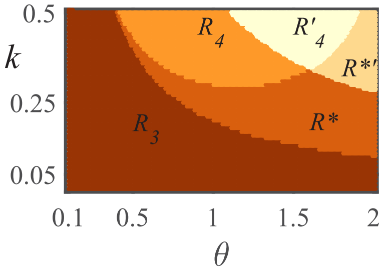

FIG. 6. Two parameters bifurcation on the θ-k plane. Equilibrium points E_3, E_4, and E^* are stable in the R_3, R_4, and R^* regions, respectively. E_4 and E^* become unstable through Hopf bifurcation and exhibit oscillations in the regions $R_4^{'}$ and $R^{*'}$, respectively.

simultaneously, and it supports our above descriptions of plankton dynamics. A phase diagram in a k-θ plane is plotted in Fig. 6 that depicts the dynamical changes of plankton populations due to simultaneous variation in nutrient enrichment (k) and the predator's preference (θ). We assume here, for simplicity, that $k_1 = k = k_2$. The parameter plane k-θ is delineated into several regions by different colors. The regions R_3, R_4, and R^* represent the stable behavior of the equilibrium E_3, E_4, E^*, respectively, and $R_4^{'}$, $R^{*'}$ represent oscillatory states of the equilibrium E_4 and E^*. It is to be noticed that zooplankton cannot withstand a low nutrient supply at any preference level. All population coexists either in a stable or in an oscillatory state as the nutrient supply increases and zooplankton inclines to PP. However, NP cannot survive if zooplankton mainly feeds on it and the nutrient supply is high. It is also noticeable that oscillatory dynamics is the only outcome if the nutrient supply (k) and zooplankton's preference (θ) to PP are both high.

The dependence of plankton dynamics on the preference parameter (θ) and mortality rate of zooplankton (d_1) is presented in another phase diagram in Fig. 7, which reveals the transitions between different states. The stability regions of the fixed points E_3, E_4, and E^* are represented by orange, yellow and red, respectively, while the white region is meant for oscillatory state. The junction of the white region to yellow and red regions is the Hopf bifurcation line. The separating lines between yellow, red, and orange regions are the transcritical bifurcation lines, where exchange of stability from one to the other equilibrium point occurs.

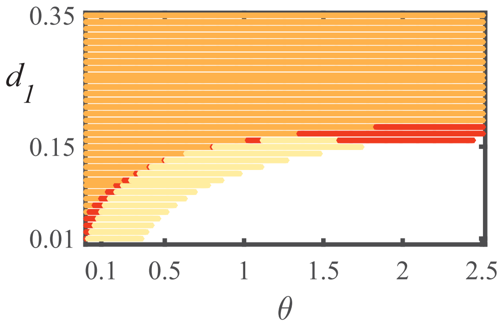

FIG. 7. Two parameters bifurcation in θ-d_1 plane. Orange, yellow, and red regions denote stable regions of E_3, E_4, and E^*, respectively. The oscillatory state is denoted by the white region.

Figure 8(a) presents a phase diagram in a k-d_1 plane that shows stable islands for different equilibrium states when zooplankton strongly feeds on NP ($\theta = 0.5$). Stability regions of E_4, E^*, and E_3 are marked by orange, red, and yellow, respectively. A second phase diagram in the k-d_1 plane in Fig. 8(b) presents stability of E_3 (dark yellow), E_4 (red), E^* (orange), and E_1 (yellow) for the choice of preference parameter $\theta = 2$. Populations are of cyclic nature in the white region.

V. DISCUSSION

It is well known that zooplankton is a selective predator [2,9] and selects its prey items depending on their nutrition value, size, digestibility, toxicity, and availability, along with others. Some studies [1,13] demonstrated that phytoplankton food quality may play a significant role in planktonic food web interactions in a pelagic ecosystem. These biological phenomena motivated us to study the dynamic consequences of the joint effects of zooplankton's selectivity and phytoplankton food quality on plankton ecosystem. To do this, we classified the entire phytoplankton population of a pelagic ecosystem into two categories: preferred phytoplankton (PP) and nonpreferred phytoplankton (NP). Phytoplanktons having superior nutrition value and that are easier to digest and nontoxic were classified as preferred prey, and phytoplanktons having inferior nutrition value, lower digestibility, and toxicity were considered as nonpreferred prey for planktivorous zooplankton. We have proposed a 3D ordinary differential equation model that incorporates zooplankton's selectivity and phytoplankton's nutritional effects in an explicit way. Phytoplankton's nutrition value was defined in terms of the reproductive gain of zooplankton. Heterogeneity of planktons at spatial and temporal scales has a profound effect on plankton dynamics and is affected by both abiotic and biotic processes [42]. To keep our model simple and analytically tractable, we did not include the heterogeneity and patchiness of plankton in our model. Circulation of water, a ubiquitous feature of the oceans, also plays an important role in forming complex spatial structures in plankton population distributions [43]. One can improve our proposed model by incorporating these biophysical characteristics. In such a case, however, the dynamic interaction depends on both time and space and requires a coupled nonlinear partial differential equation for mathematical model formulation [44]. The Diel light cycle is a controlling factor in nutrient oscillations because phytoplankton nutrient uptake is generally higher during the day than at night [45,46]. An aquatic environment, in a particular oceanic environment, is undeniably random due to physical, chemical, and biological variabilities and should be taken into account [47]. We have not even tried to fit our model with any particular data set of plankton population. Nevertheless, our study with this simplistic model is able to shed significant insights on plankton dynamics and can explain the contrasting dynamics observed in field and laboratory experiments.

Our model analysis revealed a diversity of dynamical behaviors of phytoplankton-zooplankton interaction when zooplanktons selectivity and its food quality were taken into

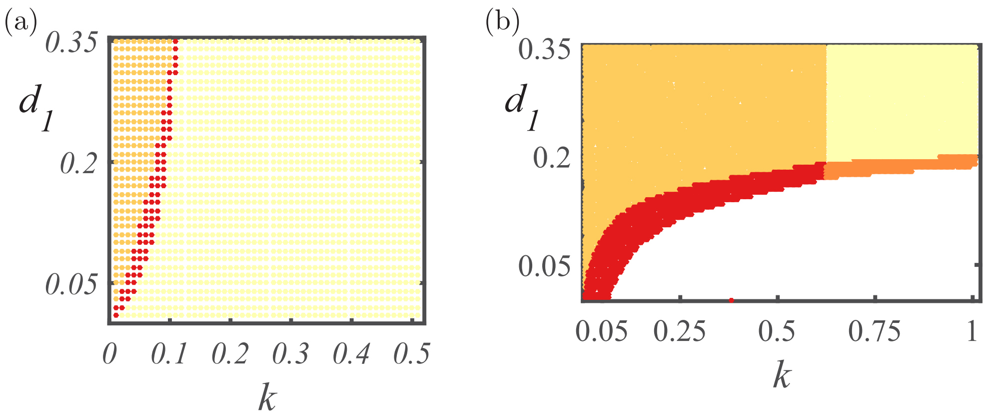

FIG. 8. Two parameters bifurcation in the k-d_1 plane for (a) $\theta = 0.5$ and (b) $\theta = 2$. (a) The orange region is for stable equilibrium E_4, red region for E^*, and yellow for E_3. (b) Dark yellow E_3, red E_4, orange E^*, yellow E_1. The white region is for limit cycle oscillations.

account. Persistent alternate blooms of all populations were observed when zooplankton strongly selected its preferred phytoplankton. This type of bloom is frequently observed in natural planktonic ecosystems. Zooplankton may switch to less nutritious nonpreferred phytoplankton due to nonavailability of its preferred prey [10–12]. In such a situation, NP may go to extinction (see Fig. 1) as its growth rate is low and zooplankton feeds preferentially on it. The biomass of zooplankton also decreases and goes to extinction due to nonavailability of its food. In absence of its predator, both types of phytoplanktons reach high density. Thus, decoupling of food chain may occur at plant animal interface if zooplankton feeds on low-nutritious phytoplankton. It has immense significance in ecosystem functioning because energy flow from a lower trophic level to a higher trophic level may be disturbed. This result gives us additional information regarding decoupling of the trophic food chain at the plant animal interface, which was generally supposed to be a consequence of intense fish predation [5].

One important characteristic of algae is its ability for rapid cell proliferation, which increases the biomass of algae, known as algal bloom. This high biomass of algae is responsible for anoxia when it is decomposed, noxious to marine ecosystems, mortality of marine life and socioeconomic damage. The bloom phenomenon has been explained by the *bottom-up* approach, where nutrients are considered as the controlling factor of algal growth [20–22]. Proponents of the *top-down* approach believe that algal bloom is regulated by its grazer [23,24]. Some others have associated bloom with the abundance of viruses [48–50] and toxic chemicals [51]. We tested the *top-down* effect on a planktonic food web through predation of zooplankton by planktivorous fish with the assumption that fish predation occurred at a rate proportional to the density of zooplankton. Density of fish population was considered as a constant because the generation time of a fish population is significantly higher than that of zooplankton. These assumptions helped us to keep the system dimension low and made the model analytically tractable. The zooplankton population always went to extinction under both types of preference if the grazing pressure was high (see Fig. 4). This result demonstrated that coupling between plants and animals was largely determined by zooplanktivour and supported the previous observations [5]. However, at a low predation rate, the stability and instability of equilibrium points depend on zooplankton's preference. NP-free stable coexistence would be the outcome at low fish predation if zooplankton strongly prefers NP. On the contrary, cyclic coexistence of NP and zooplankton was observed in the opposite preference. Coexistence of all three species was the most likely outcome for a long-range intermediate removal rate when zooplankton preferentially removed highly nutritious phytoplankton. These observations support the hypothesis that the *top-down* mechanism plays a crucial role in plankton dynamics and biomass distributions.

Eutrification, which causes many unintended consequences, is a global threat to aquatic ecosystems [49,52]. Nutrient enrichment is considered as the controlling factor of algal growth and the bloom phenomenon in a bottom-up approach. Assuming that nutrients are responsible for the variation in environmental carrying capacities [53], we have tested the *bottom-up* effect on the dynamics of phytoplankton-zooplankton interaction under different preferences of zooplankton. Recurrence multispecies blooms were the most probable outcome of the system when zooplankton feeds on highly nutritious phytoplankton with increasing nutrient availability (see Fig. 5). This is the well-known paradox of enrichment [30], which is a special case of the *principle of energy flux* [54]. It says that an increase in energy flux by means of nutritional enrichment will destabilize an otherwise stable predator-prey system. If zooplankton feed on low-nutritious phytoplankton, then E_4 or E_3, or E^* became stable in succession as the availability of nutrients was gradually increased. It was interesting to note that even under higher nutrient availability all populations coexisted in a stable state, and thus the paradox of enrichment was not observed if the zooplankton feeds on low-nutritious phytoplankton. Thus, whether a predator-prey (zooplankton-phytoplankton) system will show the paradox of enrichment or not depends on the nutritional value of the prey and the preference of the predator. This may explain the reasons why some predator-prey systems show the paradox of enrichment [4] and others do not [32]. Our study thus demonstrated various observed phenomena in plankton ecosystem, some of which are known, and some others can be tested for verification.

VI. CONCLUSION

Our study reveals that the outcome of phytoplankton-zooplankton interaction is an interplay of selective predation of zooplankton, nutritional value of phytoplankton, and grazing pressure on zooplankton. Our observations support some previous results that coupling between plants and animals is determined by the zooplanktivorous. In addition, we observed that this phenomenon may also be seen in other situations where zooplankton, in the absence of its preferred prey, switches to nonpreferred phytoplankton, whose nutritional value is low, and/or where zooplankton feeds on less nutritious phytoplankton, whose intrinsic growth rate is low. Nutrient enrichment can destabilize an otherwise stable system if predators feed preferably on highly nutritious prey, but unable to destabilize it if feeds on low-nutritious prey. This observation may be one of the possible answers to the question: Why do some experiments show the paradox of enrichment and others do not?

Besides several interesting observations on the predator-prey evolution and their relevance in respect to growth, survival, and extinction of species, we record some interesting dynamical features, such as the transcritical bifurcation of the limit cycle and transcritical bifurcation of steady state. In particular, during the transcritical bifurcation of the limit cycle, we observed a transition from a complete oscillatory state of the system to a partial oscillation, where one of the three state variables goes to death or extinction. Furthermore, during this bifurcation, we noted a transition from a relaxation-type oscillation to simple periodic oscillation. This transcritical bifurcation is well known in the literature, but its expressions are not usually seen in paradigmatic dynamical systems. From this perspective, this system itself is an interesting reservoir of dynamics to explore from a purely dynamical system viewpoint. Acknowledging several approximations and limitations, our model still reveals interesting dynamical features, such as decoupling phenomena and the paradox of enrichment, and derives conditions for coexistence and partial coexistence of species. We expect that this study will further motivate ecologists for experimental validation of puzzling phenomena in plankton populations.

ACKNOWLEDGMENTS

This research is supported by the DST(India)/SERB, Reference No. EMR/2016/001078; S.K.D. acknowledges support by the University Grants Commission (India) under the Emeritus Fellowship scheme. The authors appreciate very useful suggestions and comments by Ulrike Feudel, University of Oldenburg, Germany, and by the anonymous reviewers.

---

[1] W. R. DeMott, Limnol. Oceanography **34**, 140 (1989).
[2] J. T. Lehman, Limnol. Oceanography **21**, 501 (1976).
[3] M. A. Leibold, Evol. Ecol. Res. **1**, 73 (1999).
[4] J. M. Tubay *et al.*, Sci. Rep. **3**, 2835 (2013).
[5] J. L. Brooks and S. I. Dobson, Science **150**, 28 (1965).
[6] A. Mitra *et al.*, Prog. Oceanogr. **129B**, 176 (2014).
[7] D. T. Marleen *et al.*, J. Exp. Mar. Biol. Ecol. **343**, 210 (2007).
[8] W. R. DeMott, Limnol. Oceanogr. **33**, 397 (1988).
[9] J. Pal *et al.*, OnLine J. Biol. Sci. **10**, 11 (2010).
[10] N. Aberle *et al.*, Freshwater Biol. **50**, 369 (2005).
[11] M. E. Goecker and S. E. Kall, J. Sea Res. **50**, 309 (2003).
[12] T. Kiorboe *et al.*, Mar. Ecol. Prog. Ser. **143**, 65 (1996).
[13] M. G. Danielsdottir *et al.*, Hydrobiology **589**, 29 (2007).
[14] M. Huntley, P. Sykes, S. Rohan, and V. Marin, Mar. Ecol. Prog. Ser. **28**, 105 (1986).
[15] R. S. Fulton and H. W. Paerl, Limnol. Oceanogr. **32**, 634 (1987).
[16] G. A. Paffenhofer and K. B. Van Sant, Mar. Ecol. Prog. Ser. **27**, 55 (1986).
[17] M. van Baalen, V. Křivan, P. C. J. van Rijn, and M. W. Sabelis, Am. Nat. **157**, 512 (2001).
[18] S. F. Sailley *et al.*, J. Plankton Res. **37**, 519 (2015).
[19] J. T. Turner and P. A. Tester, Limnol. Oceanogr. **42**, 1203 (1997).
[20] J. W. Pitchford and J. Brindley, J. Plankton Res. **21**, 525 (1999).
[21] A. M. Edwards and J. Brindley, Bull. Math. Biol. **61**, 303 (1999).
[22] N. Abrantes *et al.*, Acta Oecologica **29**, 54 (2006).
[23] D. L. DeAngelis, *Dynamics of Nutrient Cycling and Food Webs* (Chapman & Hall, London, 1992).
[24] J. E. Truscott and J. Brindley, Philos. Trans. R. Soc. Lond. A **347**, 703 (1994).
[25] R. J. Diaz and R. Rosenberg, Science **321**, 926 (2008).
[26] B. J. M. Bohannan and R. E. Lenski, Am. Nat. **153**, 73 (1999).
[27] M. H. H. Stevens and C. E. Steiner, Freshwater Biol. **51**, 666 (2006).
[28] J. Slavik *et al.*, Ecology **85**, 939 (2004).
[29] P. A. Slaney *et al.*, in *Nutrients in Salmonid Ecosystems: Sustaining Production and Biodiversity*, edited by J. Stockner (American Fisheries Society, Bethesda, MD, 2003), pp. 111–126.
[30] M. L. Rosenzweig, Science **171**, 385 (1971).
[31] S. Ohno and K. Nakata, *Ecosystem Model Application to Lake Hamana-Sanaru, Coastal Lagoon System*, OCEANS 2008, Quebec City, QC, 2008, pp. 1–10.
[32] E. McCauley and W. W. Murdoch, Nature (London) **343**, 455 (1990).
[33] S. Roy and J. Chattopadhyay, J. Biosci. **32**, 421 (2007).
[34] S. R. Hall, M. A. Duffy, and C. E. Cáceres, Am. Nat. **165**, 70 (2005).
[35] N. Bairagi and D. Adak, Ecol. Complex. **22**, 1 (2015).
[36] W. W. Murdoch *et al.*, Ecology **79**, 1339 (1998).
[37] M. Genkai-Kato and N. Yamamura, Proc. R. Soc. Lond. B **266**, 1215 (1999).
[38] S. Roy *et al.*, Bull. Math. Biol. **68**, 2303 (2006).
[39] A. Mitra and K. J. Flynn, Biol. Lett. **2**, 194 (2006).
[40] See Supplemental Material http://link.aps.org/supplemental/10.1103/PhysRevE.99.012406 for stability analysis of equilibrium points.
[41] W. J. Van De Bund and E. Van Donk, Freshwater Biol. **47**, 2380 (2002).
[42] P. Pinel-Alloul, Hydrobiologia **300**, 17 (1995).

[43] A. P. Martin, Prog. Oceanogr. **57**, 125 (2003).
[44] A. B. Medvinsky *et al.*, Phys. Rev. E **64**, 021915 (2001).
[45] I. Tsakalakis *et al.*, Ecol. Model. **384**, 241 (2018).
[46] J. B. Heffernan and M. J. Cohen, Limno. Oceanogr. **55**, 677 (2010).
[47] P. F. J. Lermusiaux, J. Comp. Phys. **217**, 176 (2006).
[48] C. P. D. Brussaard, J. Eukuryor. Microbiol. **51**, 125 (2004).
[49] Z. A. D. Sarno and G. Forlani, J. Plankton Res. **21**, 2143 (1999).
[50] S. Ruan, J. Theor. Biol. **208**, 15 (2001).
[51] J. Chattopadhyay *et al.*, J. Theor. Biol. **215**, 333 (2002).
[52] J. M. Davis *et al.*, Proc. Natl. Acad. Sci. U. S. A. **107**, 121 (2010).
[53] K. L. Cottingham *et al.*, Ecol. Lett. **3**, 340 (2000).
[54] J. M. K. Rip and K. S. McCann, Ecol. Lett. **14**, 733 (2011).